UV, VISIBLE, AND INFRARED SPECTRAL EMISSIONS IN HYBRID ROCKET PLUMES

M. Keith Hudson, Robert B. Shanks, Dallas H. Snider,
Diana M. Lindquist, Chris Luchini, and Sterling Rooke

Department of Applied Science
University of Arkansas at Little Rock
2801 S. University
Little Rock, AR 72204

Abstract

A survey was made of the spectral emissions from a 2 x 10 inch labscale hybrid rocket motor system. The emissions in the Ultraviolet-Visible (300-750 nm), Near Infrared (750-1100 nm), and Mid Infrared (2-16 μm) regions were studied. Baseline emissions were found to consist of the sodium and potassium atomic lines, present due to the use of silica phenolic insulators, and the C_2, OH, and CH combustion bands. Doped fuel studies were performed, using hydroxyl-terminated polybutadiene (HTPB) fuel mixed with metal salts to introduce emitters into the plume. Metals studied included manganese, nickel, cobalt, copper, and iron. Iron was studied in both the II and III oxidation states. Manganese was also used to study the effect of concentration, and indicated that plume emission is quantitative, giving linear output for the range 5 to 40 ppm. Overall, the labscale hybrid was found to offer a stable system for plume spectroscopy, whether for direct studies of the hybrid type rocket, or for use in plume simulations of other propulsion systems.

Introduction

The hybrid rocket motor is of interest to the aerospace community for several reasons. Two of these, the possible use of hybrids as boosters and their potential usefulness as a plume simulator for other rocket systems, particularly solids, indicate the need for a thorough survey of their spectroscopic emissions. For potential use as boosters, which has been discussed as possible alternatives to the current Space Shuttle Solid Rocket Motors (SRM), hybrids must be evaluated as to base heating effects, which are related to total IR emissions. The hybrid also appears to be an excellent motor system to use in ground based testing, especially for the general development of optical monitoring and other measurement techniques. A properly designed system, built from the ground up for these types of applications, offers an attractive and safe alternative to the use of solid or liquid propellant systems.[1] This paper reports the results of a spectral study of such a hybrid system.

Atomic Emission Spectroscopy

An atomic emission system basically consists of a source into which a sample can be introduced, a wavelength selector, and an optical detector. The system used in this study is typical of those used for most emission experiments, but the source of emissions, a labscale hybrid motor, is different in several ways from those normally utilized.

As a base for comparison, the ideal atomic emission source has the following characteristics:

1. Complete atomization of all elements.
2. Controllable excitation energy.
3. Sufficient excitation energy to excite all elements.
4. Inert chemical environment.
5. No background.
6. Will accept solutions, gases, or solids.
7. Tolerant to various solution conditions and solvents.
8. Simultaneous multielement analysis.
9. Reproducible atomization and excitation conditions.
10. Accurate and precise analytical results.

The hybrid rocket plume does provide a high energy source for the atomization and excitation of the elements involved. The plume temperature has been measured to be approximately 2500-2700 degrees C, which is about the same as a hydrogen-air flame.[2] The temperatures in the combustion chamber are even higher, on the order of 3000 degrees C, providing more energy for the atomization process. The combustion stoichiometry is set to be fuel lean, which normally should provide lower background emissions. Rocket plumes in general then do supply an environment which is capable of good atomization and excitation, and can provide these to solids liquids or gases presented to the combustion chamber. Also, the motor control system allows precision metering of the oxidant, rigidly setting the operating point of the motor when fired. This renders good reproducibility in firing conditions, which, along with fuel dopant seeding homogeneity, results in reproducibility between firings.

However, it is obvious that a rocket plume falls short on several of these characteristics. Since the only method currently available for sample introduction is doping of the fuel grain, this limits us to metals, metal salts, or other solids, which then must not react with the polymer fuel while curing. Hybrid motors display a significant amount of particulate matter in the plume, therefore, there is a component of blackbody type background radiation. The plume is exposed to the atmosphere, which is not an inert chemical background, but allows additional oxidant to react with exhaust gases. Characteristically, hybrid motors have an inherent tendency to pressure oscillations, on the order of 20-60 Hertz.[3,4] This causes fluctuations in plume intensity. However, these fluctuations can normally be averaged or integrated out in the detection process, when using the "standard" atomic spectroscopy PMT or array detectors.

Experimental

Hybrid Rocket Facility

A hybrid rocket testing facility, complete with a computer control and data acquisition system, was designed and constructed for spectroscopic studies of the hybrid rocket motor plume and its use as a simulator for solid and possibly liquid motor systems. This facility has been described in another paper,[5] but certain aspects will be discussed here since they affect

spectroscopic data collection. The hybrid rocket motor used in this study was a two by ten inch system, capable of firing at pressures to approximately 500 psi. It was fitted with pressure and temperature transducers to record these parameters with respect to time; during startup, run, and shut-down. Pressure data was collected at 1000 Hz and is of particular interest since it indicates any transients or unusual conditions present during a firing. This pressure data was recorded and presented in such a form as to allow ease of utilization with data from the various spectroscopic systems employed in the study. Also, the hybrid motor was set up to allow full access to any particular point in the plume for spectral study. This was particularly important when using spatial imaging systems, such as standard video and IR thermal units.

Instrumentation

Two systems were used for spectral monitoring of the ultraviolet and visible spectral regions. A Princeton Applied Research Optical Multichannel Analyzer (OMA) Model III, which included a .33 meter ISA Spectrograph, was used in all of the firings studied. This unit was used as a high resolution instrument, in a layout similar to previous studies.[6] Slit width was set at 12 micrometers and a 5 meter fiber optic was used for light collection. Another system, assembled in our laboratory, was used in many of the firings. This unit included a Spex Model 270M Spectrograph using a Reticon 1024S linear array detector in the focal plane and a 486-33 PC computer set up to control the array and collect data.[7] This system was used in a lower resolution mode, monitoring both lines and bands, by setting the slit width at 100 micrometers. This instrument was placed in close proximity to the plume under study, using a single lens for light collection.

For IR spectral monitoring, a Midac FTIR Emission Spectrometer with 2-16 micrometer spectral response mercury cadmium telluride (MCT) broadband detector was used. The spectrometer was fitted with an adjustable iris at the entrance aperture to limit the amount of light entering the unit. The FTIR used a 486-33 portable PC computer for data collection and storage. A separate 486-50 PC computer was used to analyze this data, as it provided greater display versatility. Software was written in house to control this instrument and provide data display and manipulation capability. Further IR monitoring was performed with an Inframetrics Model 600 IR Camera. This system was used for thermal imaging of the rocket chamber, nozzle, and plume.

Materials

Fuel for the hybrid motor used in these studies was hydroxyl-terminated Polybutadiene (HTPB), using Desmodur N-100 or similar isocyanates for curatives. Standard tanks of industrial grade oxygen were used as the oxidant in all studies. Internal chamber materials which could affect overall spectral emissions included silica phenolic insulators in the fore and aft chamber areas, a paper phenolic fuel grain insulator sleeve, the motor's graphite nozzle, and portions of exposed stainless steel surfaces in the injector head.[5] Some firings at the end of the reported study were done using graphite fore and aft insulators to determine the effect of the silica phenolics.

Dopants were used in this study to establish the feasibility of using labscale systems for plume diagnostics and spectral simulations. These dopant metals included nickel, iron manganese,

copper, and cobalt. Specific compounds used were manganese chloride tetrahydrate, nickel chloride hexahydrate, and cobalt chloride hexahydrate. Dopants were introduced in the hybrid plume by mixing them into the fuel material prior to grain casting. The amount was calculated to give the desired concentration in the plume, with the calculation including the fuel amount from regression rate data and oxidant amount from the mass flow rate settings. Plume concentrations from 10 to 200 ppm were used in this study.

Results and Discussion

Baseline Spectral Studies

UV-Vis Spectral Region

Emissions in the UV-Vis spectral region may be in the form of atomic line emissions or as molecular band emissions. Both types of spectral emissions were seen during our study of the hybrid plume. Initially, work focused on a survey of the hybrid motor baseline emissions in order to characterize the overall system for later use in simulations and diagnostics testing. Also, this data should provide a general baseline for all hybrid motors, as long as fuel differences and the components used in a particular system and their probable contribution to the spectral signature are considered. Runs were made at O/Fs of 2.9 to 3.0, with an oxidizer mass flow of 0.1000 lbm/sec.

Two atomic emitters were found in the labscale hybrid rocket plume. Atomic lines were detected for sodium at 589 nm (doublet) and for potassium at 404 nm and in the 760 nm range. Figure 1 shows the emission from sodium with respect to burn duration. Note that the line intensity shows ignition and a portion (2.1 seconds) of the constant burn of the motor. Data for potassium was very similar. From the literature, it is found that these alkali metals are among the most easily thermally excited emitters known, and are present as contaminants in almost any material.[8] While the HTPB and curative almost certainly have at least trace amounts of these metals in them, a more common source of sodium and potassium in these levels is the glass or silica phenolic. Glass typically has these elements present in large enough quantities to give these signature line emissions, especially when the sacrificial character of the glass phenolic is recognized. Most of the emission from these two sources then is expected to result from the silica phenolic insulators, especially from the aft insulator, as it ablates dramatically during firings. Figure 2 shows the strong emission lines found for potassium at 766.4 and 769.8 nm during steady burn conditions, in the middle of a firing, and is typical of the intensity seen for both metals. Potassium was also seen at 404 nm during high resolution monitoring of a dope fuel grain. The intensity of this emission was significantly lower than that for the 760 region, and it was not initially noted in low resolution studies. No other atomic emissions were found in the UV-Vis region during any baseline HTPB firings, demonstrating that contributions to hybrid emissions from other metals are insignificant. This implies that other metal emitters which might modify the spectral output of the hybrid plume are only present in the HTPB fuel and ablative motor components in trace amounts, if at all.

A brief set of experiments were carried out using graphite insulators instead of the original silica phenolic design. Spectra for these firings lacked the rather large intensity peaks as seen for sodium and potassium, although a low level sodium line can be detected. This data supports the hypothesis that the sodium and potassium seen in the earlier firings were a result of ablation of the glass type insulators, and that those insulators were responsible for the great majority of atomic line emissions.

Molecular emissions from the hybrid motor included several bands that are expected in the combustion of hydrocarbons. Emissions from C_2, CH, and OH were found. C_2 emissions were found centered at 463, 509, and 559 nm. CH emissions were noted centered at 382 and 427 nm. The OH band is visible from 308 to 320 nm. These bands are also seen in methane, propane, and fuel gas monitoring, with OH also found in studies and monitoring of LH2/LOX engines.[9,10] The presence of these bands support the use of hybrids as simulators for diagnostics development for other rocket propulsion systems.

An overall rise in background signal was noted for almost every firing. The shape and intensity of this emission was consistent with the ejection of hot particulate matter in the exhaust plume, giving rise to blackbody emission. Firings performed with a carbon black opacifier seemed to confirm this finding, as the blackbody background emission intensified during these runs from increased plume particulate loading. Another indication of this particulate content was the higher level of background emission at the end of firings, as oxidant levels were decreasing in the motor chamber. This is consistent with a fuel-rich condition, which would also increase particulate loading of the plume at that time.

IR Spectral Region

Figure 3 shows a plot of the major emission intensity, found between 2 and 5 micrometers, resulting from the firing of HTPB fuels in the hybrid system. The bands present are those of water vapor, centered at about 2.7 μm, and carbon dioxide, at about 4.4 μm. The HTPB hydrocarbon polymer burns predominantly to the products water and carbon monoxide, with the carbon monoxide being afterburned to carbon dioxide after passage through the nozzle and subsequent entrainment of atmospheric oxygen. Close examination of the 2 to 5 μm spectrum does show a small set of peaks at approximately 4.7 to 4.9 μm. These peaks are tentatively identified as belonging to carbon monoxide. They are not seen in many of the scans taken, and their presence may be a function of motor burn conditions, such as those found during motor ignition or shut-down. Further studies will be required to identify these peaks and their cause.

The detector used in this study allowed the collection of data between 2 and about 16 μm, and other bands were noted beyond those reported above, although all were of lesser intensity. However, all of these bands were also characteristic of water vapor and carbon dioxide. In many cases, these bands were obscured by microphonic noise effects apparently coupled into the interferometer section of the FTIR. Figure 4 shows these emission bands for a selected firing, with minimal microphonics. Water vapor bands are seen between 5 and 6 μm and again in the 6-8 μm region. Carbon dioxide is seen at 14-15 μm, although this band appears somewhat modified

by microphonics. Note that this is a "raw" spectrum, uncorrected for detector response, and emphasizes the intensity of these longer wavelength peaks.

IR imaging gave results similar to those obtained observing solid plumes, with the IR imaged plume appearing larger than when viewed by standard video or by the naked eye. Shock diamond structure was visible in more detail than when using standard video. Chamber heating was shown to affect only the nozzle end of the motor, with the grain and injector head portion of the motor remaining cool.

Doped Fuel Spectral Studies

A series of firings utilizing metal seeded fuel grains were carried out at concentrations calculated for in-the-plume levels of 10 to 200 ppm dopant. The exact concentration depended on considerations of the relative emissivity of the metal used, as known from spectral references and prior studies on a liquid fueled test thruster.[6,8,10] These firings also included metals which exhibit different oxidation states, with compounds for both states being used to ascertain any differences in spectral emissions. All studies in this series were again carried out at an oxidant-to-fuel ratio (O/F) of between 2.9 and 3.0, with oxidizer mass flow of 0.1000 Lbm/sec. The five metals used in the study were chosen since they represent common alloy metals found in turbine pumps as used in the SSME.[10] The same type of pumps could be used in the oxidant supply system of a flight hybrid motor. The figures following give the observed wavelengths, the identified emitters, and the corresponding literature wavelengths.[11]

Figures 5 and 6 are the spectra resulting from the introduction of 10 ppm manganese into the hybrid plume. This metal resulted in the greatest signal-to-noise (S/N) ratio observed for the dopant metal studies. S/N is estimated at approximately 10 for the highest peak in the high resolution spectrum, Figure 6. Also noted for the manganese doped firings were several bands identified as originating from Mn(OH).[9] These bands are identifiable in Figure 5, collected using the low resolution system. Figure 7 shows the spectrum obtained for nickel at a concentration of 100 ppm. S/N levels for the peaks observed varies between about 3 and 5 for this spectrum. Figure 8 is the spectrum for cobalt at 100 ppm concentration. S/N is very similar in magnitude to that obtained for a grain containing copper sufficient to give 20 ppm metal concentration in the plume, shown in Figure 9.

Iron was chosen to study the effect that compounds of different oxidation states might have on the plume spectra. Figure 10 shows the spectrum for iron(II) at 100 ppm plume concentration. A grain containing iron(III) was fired under the same conditions and resulted in a smaller signal. Another grain, containing 200 ppm iron(III) was made and fired, with results similar to the iron(II) spectrum shown.

Quantitation Study

The concentrations of elemental manganese in the plume used in this study ranged from 5 to 100 ppm. This corresponds to concentrations of manganese chloride in the fuel grain of 45 to 900 ppm, as shown in Table 1. These values assume an oxidizer mass flow of 0.1000 lbm/sec and a fuel grain of 450 grams. These firings were set up to utilize a fuel lean condition compared to stoichiometric combustion to CO, which occurs at an O/F of 2.074. Conditions were set for an O/F of 2.29, used in all firings in this experimental subset.

A base line spectra for a HTPB fuel grain is shown in Figure 11. A small doublet is noted at approximately 404.5 nm, corresponding to the potassium doublet, present as an impurity in the fuel grain. Nine levels of dopant were used, 5, 10, 15, 22, 40, 55, 70, 85 and 91 ppm. After the fuel grains were doped with the appropriate amount of manganese chloride, they were fired for three seconds each. This gave approximately ten scans of clean spectra to work with, as it was found that the first two and last two scans during the firing were not usable due to start up and end transients in the firing. To quantify the data the peak at 403.4 nm was used. This peak is actually made by two contributing lines at 403.31 and 403.45 nm. The peak heights were measured relative to the base line. This was measured for each scan and then averaged for the run. Figure 12 shows how the peak heights were measured. Figure 13 shows a typical plot of data collected for an entire firing and Table 2 shows all of the data collected for the study.

A curve was fit to the data, as illustrated in Figure 14, showing the relative emission levels were observed to be nearly linear over the low concentration regime (5 to 40 ppm). This fits with the basic theory of atomic emission. The curve flattens out at higher concentrations, probably due to self-quenching. The large size of the error bars gives a clue to the amount of aberration due to using the rocket plume as the source. These fluctuations in peak height for a given firing could be due to several factors. The first hypothesis is that the pressure oscillations in the rocket chamber are causing the plumes emissivity to change with time. The second hypothesis is that the concentration of dopants in the plume is actually varying during the firing. This could be caused by two factors. The first is that the dopants are for some reason not distributed homogeneously in the fuel grain. The second is that the hybrid rocket combustion characteristics are unique, due to the interaction of the gaseous oxidizer and combustion products with the solid fuel surface. It has been speculated that the solid fuel surface builds up a char layer, which sometimes sheds, causing an avalanche effect of charred material. This could be causing a higher particulate count in the plume, changing its emissivity, or contributing more dopant to the plume causing the variation in concentration.

Conclusions

The labscale hybrid motor offers a stable plume for spectral studies in several areas. It can be used as a tool for hybrid motor characterization, as a simulator for solid rocket motors, and as a platform for instrumentation development. The fuel grain can be seeded with materials to simulate failure modes in liquid engines and larger scale hybrids, or to produce plumes which allow the study of possible fuel additives. While not as spectrally clear as liquid fueled LH2/LOX engines, the hybrid does allow the collection of useful diagnostic data. The baseline HTPB data collected should provide a starting point for further spectral studies, both for hybrid combustion investigations and for possible hybrid system diagnostics. This study also shows that the hybrid

exhaust contains no appreciable amounts of corrosive pollutants and indicates that hybrids are environmentally clean, relative to solid motors.

Acknowledgements

The authors wish to thank the Arkansas Space Grant Consortium for initial "seed" funding of this work. We would also like to thank the NASA Stennis Space Center for the loan of equipment and NASA Grant No. NAG13-26. Dr. Shanks expresses his appreciation to NASA and the Stennis Space Center for his Graduate Student Researchers Fellowship support. Additional support was furnished through NASA Grant NCCW-0055. We would like to thank Ken Kalb, Armand Tomany, and Greg Cress for their technical skills and help in the areas of electronic, mechanical, and machining support.

References

1. Shanks, R.B., "A Labscale Hybrid Rocket and Facility for Plume Diagnostics and Combustion Studies," A Doctoral Dissertation, University of Arkansas at Little Rock, December, 1994.

2. Teague, M.W., Felix, T., Hudson, M.K., and Shanks, R., "Application of UV-Vis Absorption to Rocket Plumes," AIAA Paper No. 95-2790, July, 1995.

3. Lindquist, D., Hudson, M.K., Shanks, R., Luchini, C.B., and Rooke, S., "Infrared Emission Monitoring of Rocket Plumes," AIAA Paper No. 95-2789, July, 1995.

4. Desrochers, M., Olsen, G.W., and Hudson, M.K., "Investigation of Pressure, Plume Flicker, and Thrust in a Labscale Hybrid Rocket," AIAA Paper No. 97-3036, July, 1997.

5. Shanks, R, and Hudson, M.K., "The Design and Control of a Labscale Hybrid Rocket Facility for Spectroscopic Studies, "AIAA Paper No. 94-3016, 30th AIAA/ASME/SAE/ASEE Joint Propulsion Conference, Indianapolis, IN, June 27-29, 1994

6. Gardner, D.G., Bircher, F.E., Tejwani, G.D., and Van Dyke, D.B., "A Plume Diagnostic Based Engine Diagnostic System for the SSME", AIAA Paper No. 90-2235, 1990.

7. Snider, D.G., and Hudson, M.K. "Evaluation of Photodiode Arrays in Rocket Plume Monitoring and Diagnostics", Proc. Ark. Acad. Sci., 1994, 48, 174-180.

8. Ingle, J.D., and Crouch, S.R., Spectrochemical Analysis, Prentis-Hall, Englewood Cliffs, NJ, 1988.

9. Gaydon, A.G., The Spectroscopy of Flames, Chapman and Hall, London, 1974.

10. Tejwani, G.D., Van Dyke, D.B., Bircher, F.E., Gardner, D.G., and Chenevert, D.J., "Emission Spectra of Selected SSME Elements and Materials", NASA Reference Publication No. 1286, December, 1992

11. Weast, R.C., Ed., CRC Handbook of Chemisty and Physics, 69th ed., CRC Press, Boca Raton, FL, 1988.

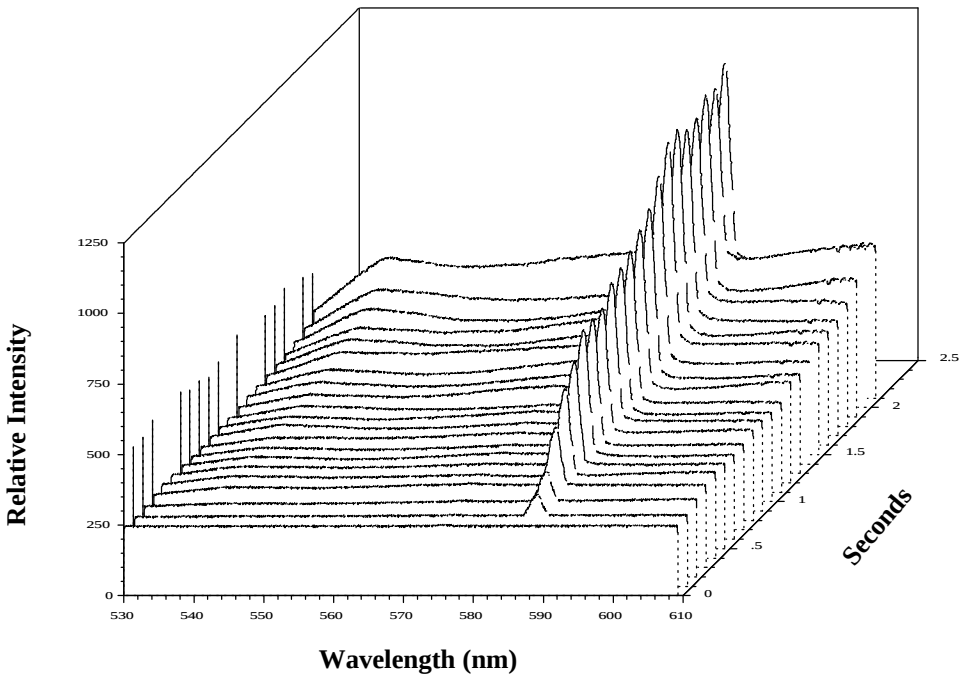

Figure 1. Cascade Plot of Sodium Emissions, Ignition to 2.1 Seconds
(Low Resolution System)

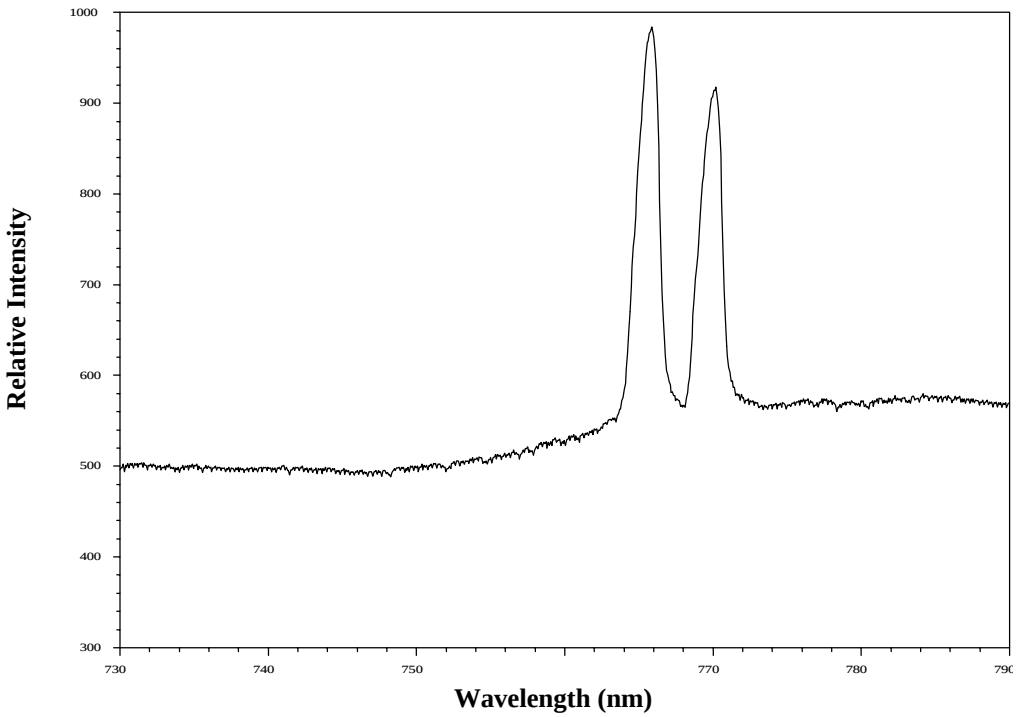

Figure 2. Potassium Emissions in the 760 nm Region
(Low Resolution System)

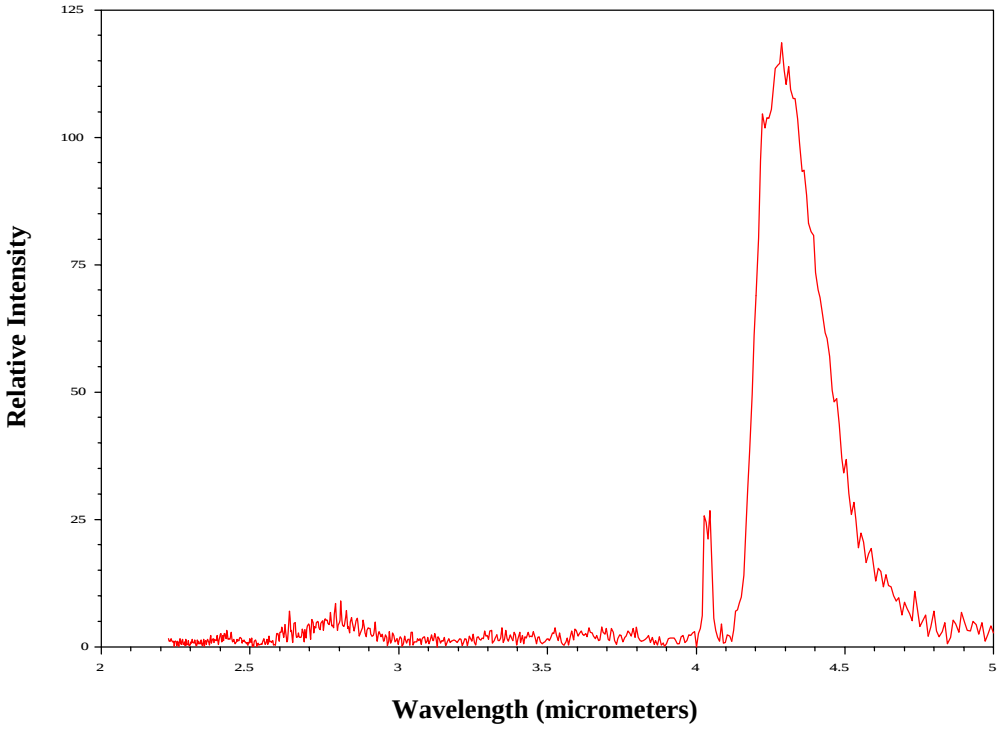

Figure 3. IR Emissions 2-5 µm Region

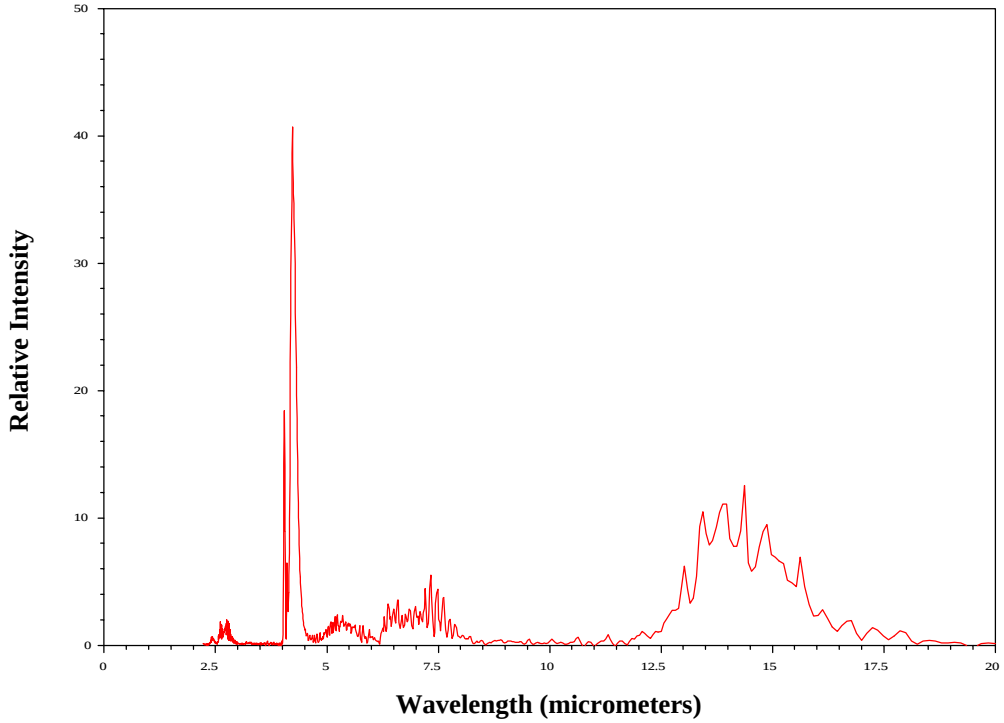

Figure 4. IR Emissions 2-16 µm Region

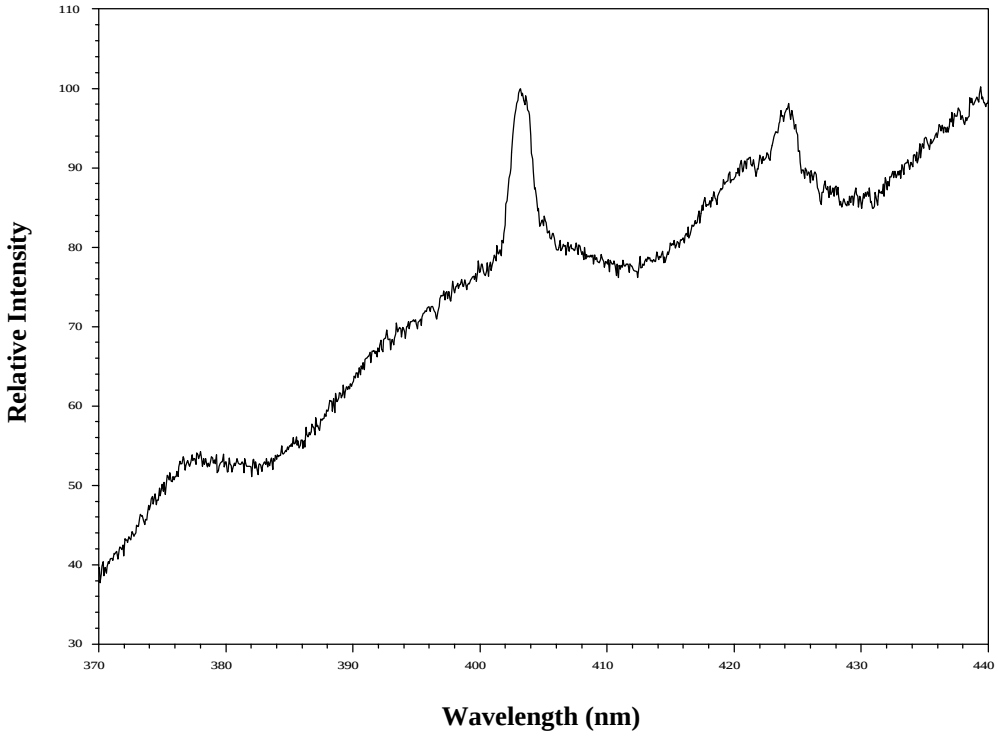

Spectral Lines and Bands for Hybrid Motor Plume Doped with 10 ppm Manganese
(Low Resolution System)

Wavelength (nm)	Emitter
378 to 383 (bands)	CH, Mn(OH)
403	Mn (two lines)
404	K (two lines)
400 to 410	Mn(OH)
418 to 426	Mn(OH)
424.5	Unknown

Figure 5. 10 ppm Manganese Firing Showing Bands and Atomic Lines
(Low Resolution System)

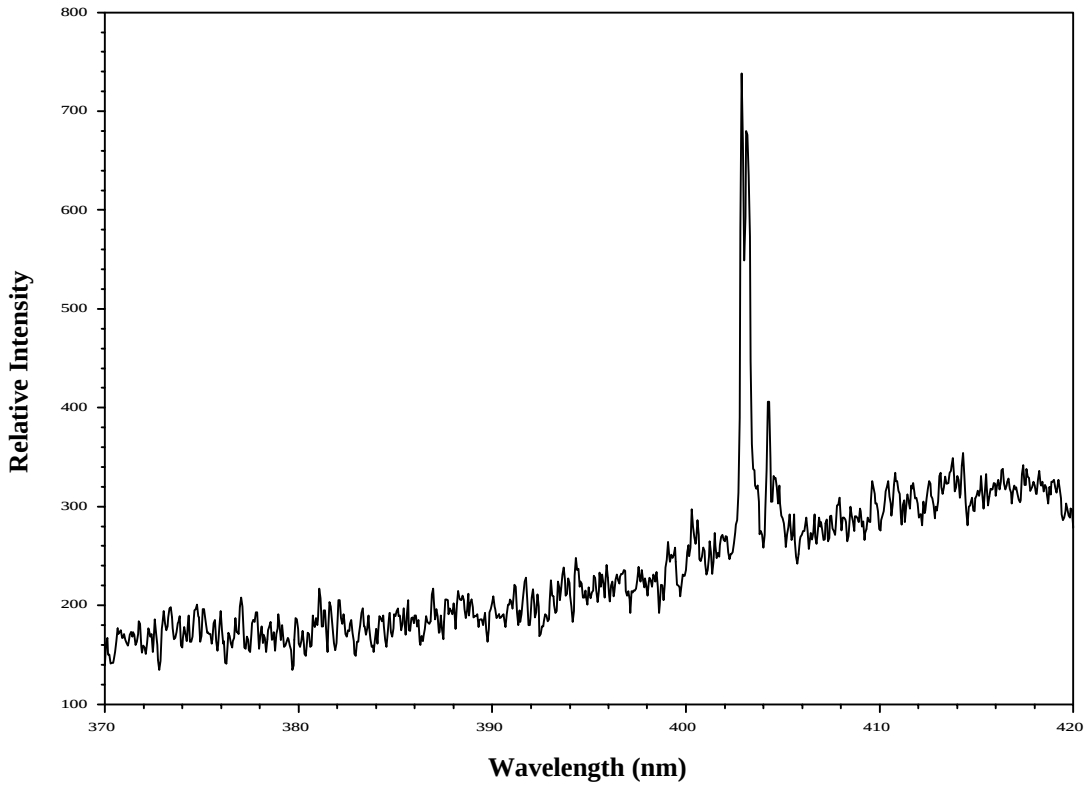

Spectral Lines for Hybrid Motor Plume Doped with 10 ppm Manganese

Wavelength (nm)	Emitter	Contributing Lines (nm)
402.88	Mn	403.08
403.14	Mn	403.31, 403.45
404.26	K	404.41
404.54	K	404.72

Figure 6. 10 ppm Manganese Spectrum
(High Resolution System)

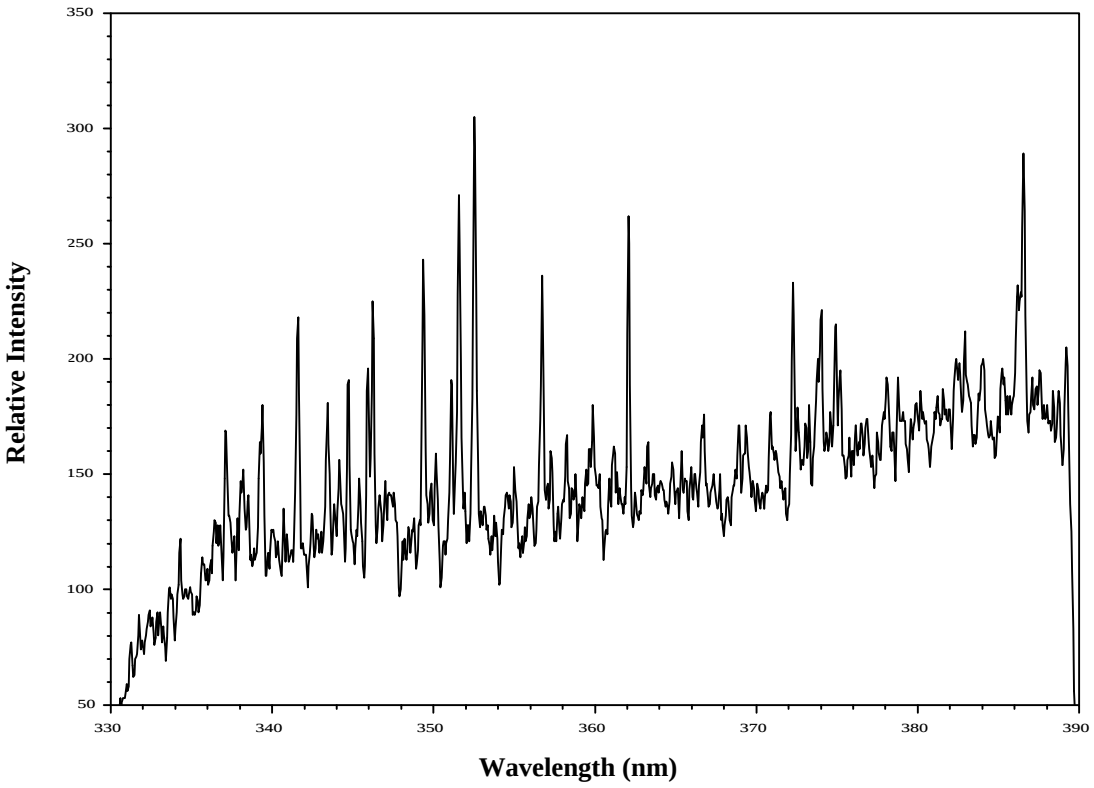

Spectral Lines for Hybrid Motor Plume Doped with 100 ppm Nickel

Wavelength (nm)	Emitter	Contributing Lines (nm)		Wavelength (nm)	Emitter	Contributing Lines (nm)
337.12	Ni	336.96, 337.20		352.51	Ni	352.45
339.4	Ni	339.11, 339.30		356.72	Ni	356.64
341.6	Ni	341.48		358.24	Ni	357.19 ?
343.44	Ni	343.36		359.86	Ni	359.77
344.72	Ni	344.63		362.06	Ni	361.94
345.92	Ni	345.85		372.26	Fe	371.99
346.22	Ni	346.17		374.02	Fe	373.71
349.37	Ni	349.3		374.9	Fe	374.83, 374.95
351.09	Ni	351.03		382.92	Ni	383.17 ?
351.56	Ni	351.51		386.54	Ni	385.83

Figure 7. 100 ppm Nickel Spectrum
(High Resolution System)

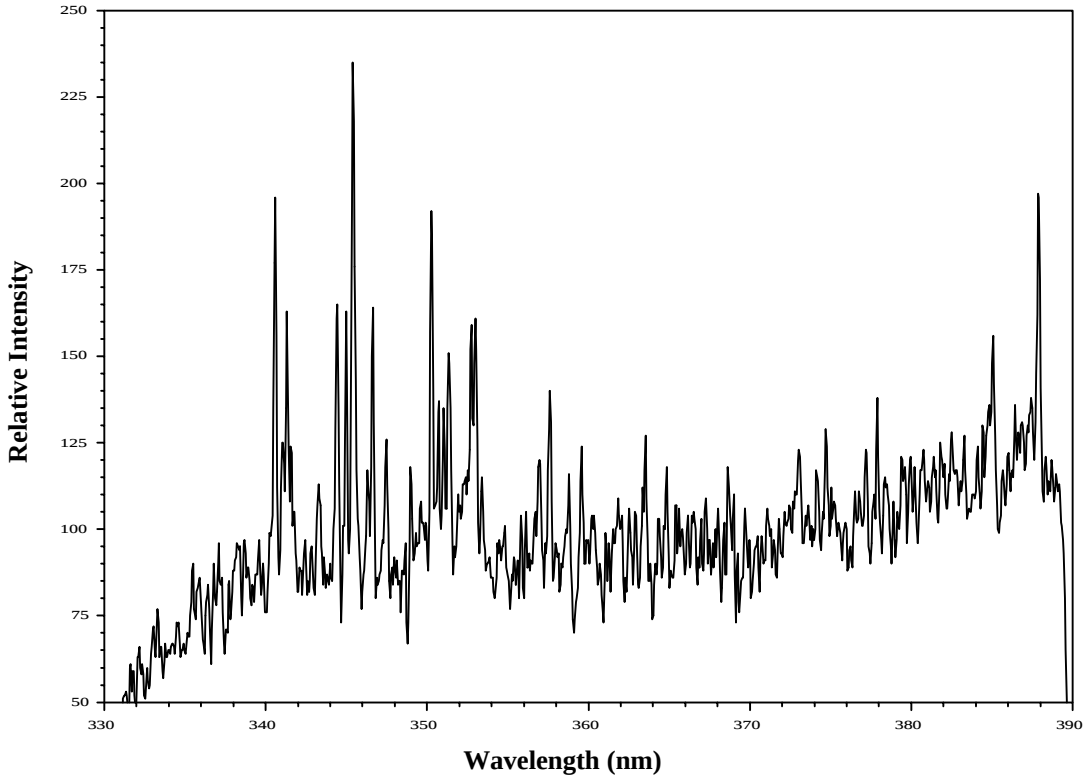

Spectral Lines of Hybrid Motor Plume Doped with 100 ppm Cobalt

Wavelength (nm)	Emitter	Contributing Lines (nm)		Wavelength (nm)	Emitter	Contributing Lines (nm)
340.58	Co	340.51		352.98	Co	352.98
341.3	Co	341.23		356.97	Co	356.94
344.44	Co	344.36		357.6	Co	357.50, 357.54
344.98	Co	344.92		358.79	Co	358.72
345.39	Co	345.35		359.56	Co	359.49
346.64	Co	346.58		363.54	Co	363.14
347.46	Co	347.4		373.02	Unknown	?
350.26	Co	350.23		374.68	Co	374.55
350.69	Co	350.63		377.88	Unknown	?
351.03	Co	350.98		385.06	Co	384.55
351.33	Co	351.26, 351.35		387.86	Co	387.31, 387.40
352.74	Co	352.69				

Figure 8. 100 ppm Cobalt Spectrum
(High Resolution System)

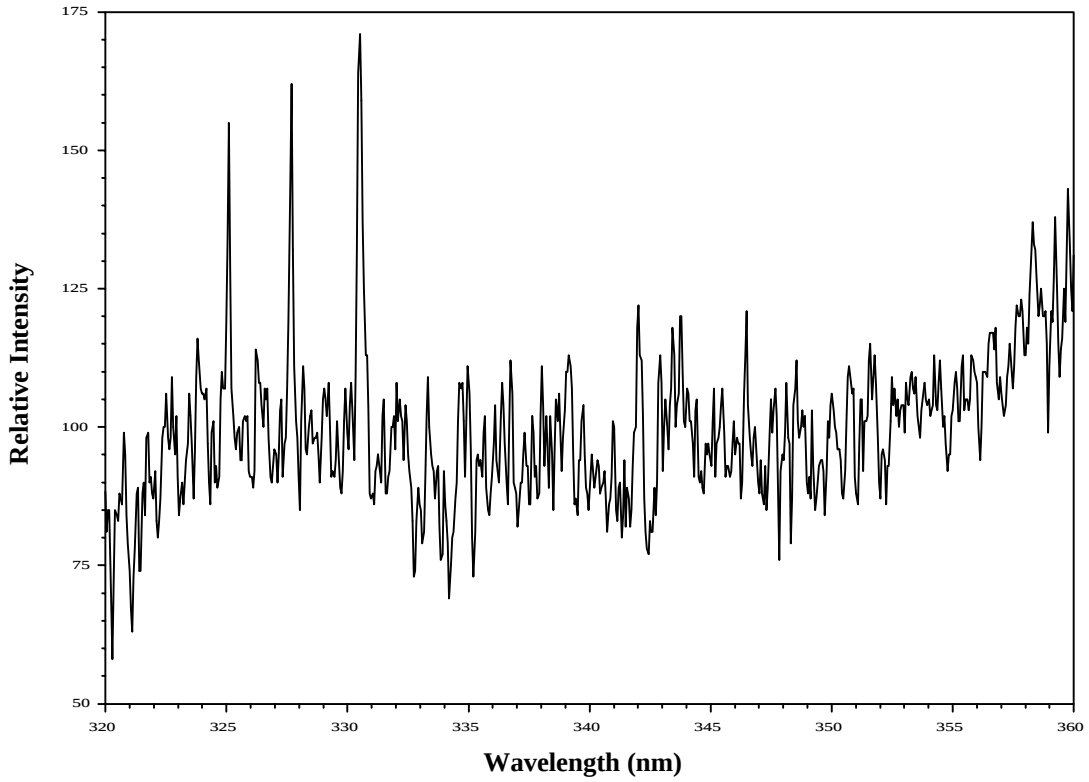

Spectral Lines for Hybrid Motor Plume Doped with 20 ppm Copper

Wavelength (nm)	Emitter	Contributing Lines (nm)
325.1	Cu	324.75
327.68	Cu	327.4
330.51	Cu	330.8

Figure 9. 20 ppm Copper Spectrum
(High Resolution System)

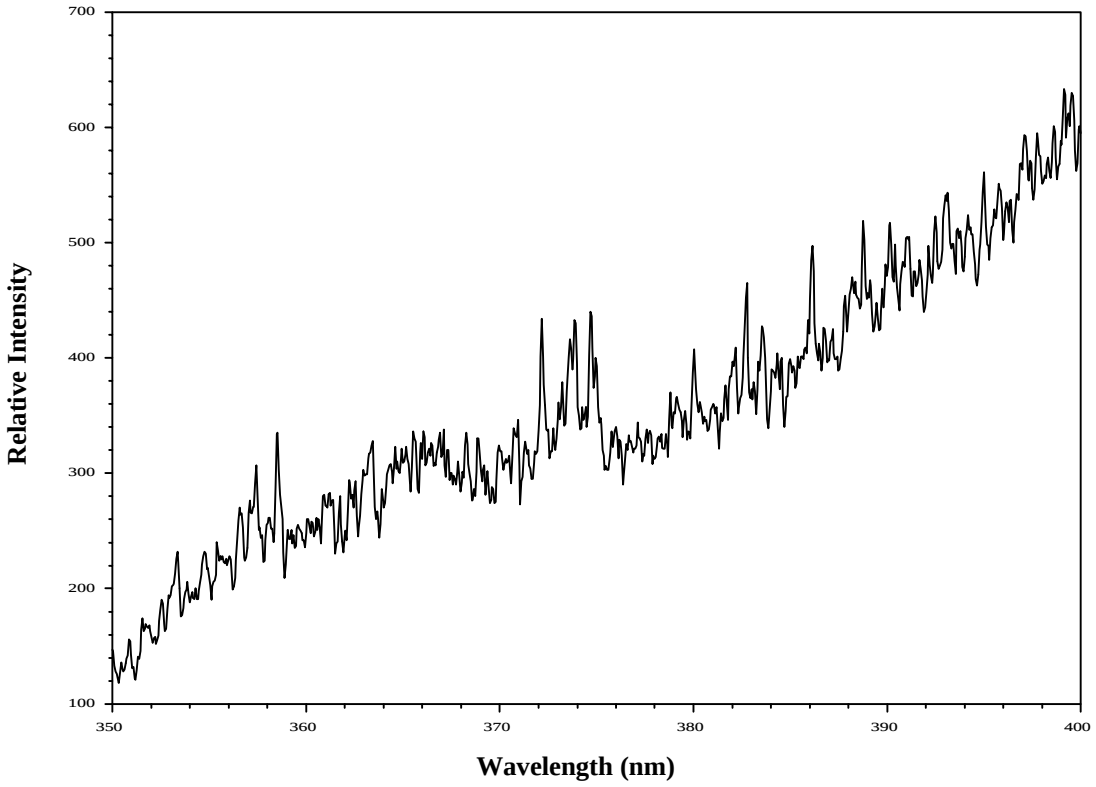

Spectral Lines for Hybrid Motor Plume Doped with 100 ppm Iron

Wavelength (nm)	Emitter	Contributing Lines (nm)		Wavelength (nm)	Emitter	Contributing Lines (nm)
357.43	Fe	357.01, 357.03		380.02	Fe	379.95
358.51	Fe	358.12		382.18	Fe	382.04
372.16	Fe	371.99, 372.26		386.14	Fe	385.99
373.62	Fe	373.49		388.76	Fe	388.63
373.88	Fe	373.71		390.14	Fe	389.97
374.66	Fe	374.56		393.02	Fe	392.79
374.96	Fe	374.83		393.13	Fe	393.03

Figure 10. 100 ppm Iron Spectrum
(High Resolution System)

Table 1. Dopant amounts for Manganese Chloride, dehydrated
(0.1344 lbm/sec total mass flow).

Desired PPM in Plume	Mass of Metal Chloride Salt Added to the 450 gram Fuel Grain
5	0.0202 grams
10	0.0403 grams
15	0.0605 grams
22	0.0887 grams
40	0.1613 grams
55	0.2218 grams
70	0.2822 grams
85	0.3427 grams
91	0.3669 grams

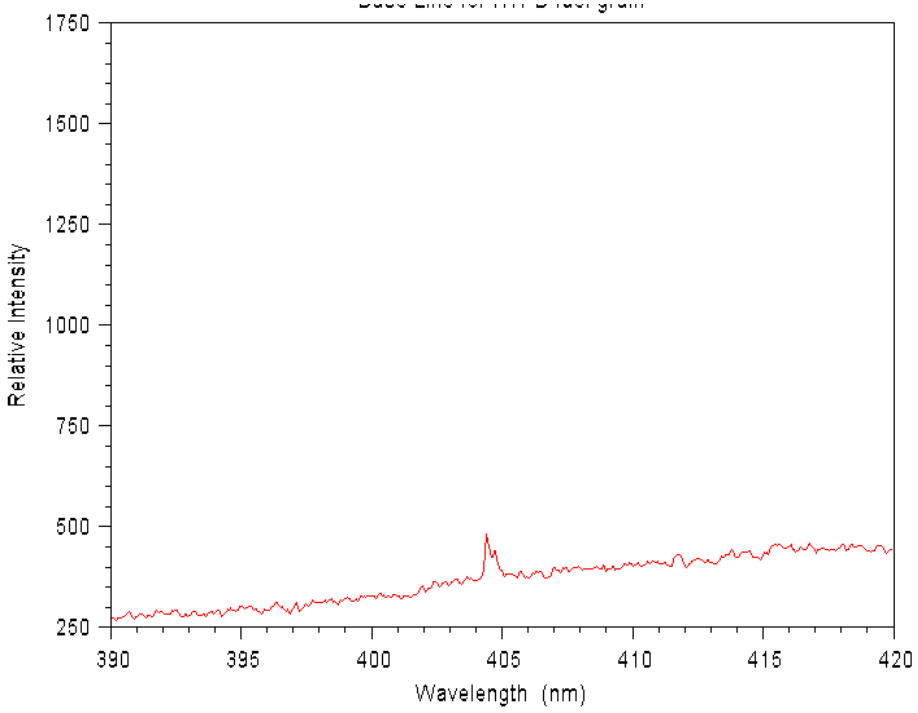

Figure 11. Baseline Data for a Non-doped HTPB Fuel Grain.

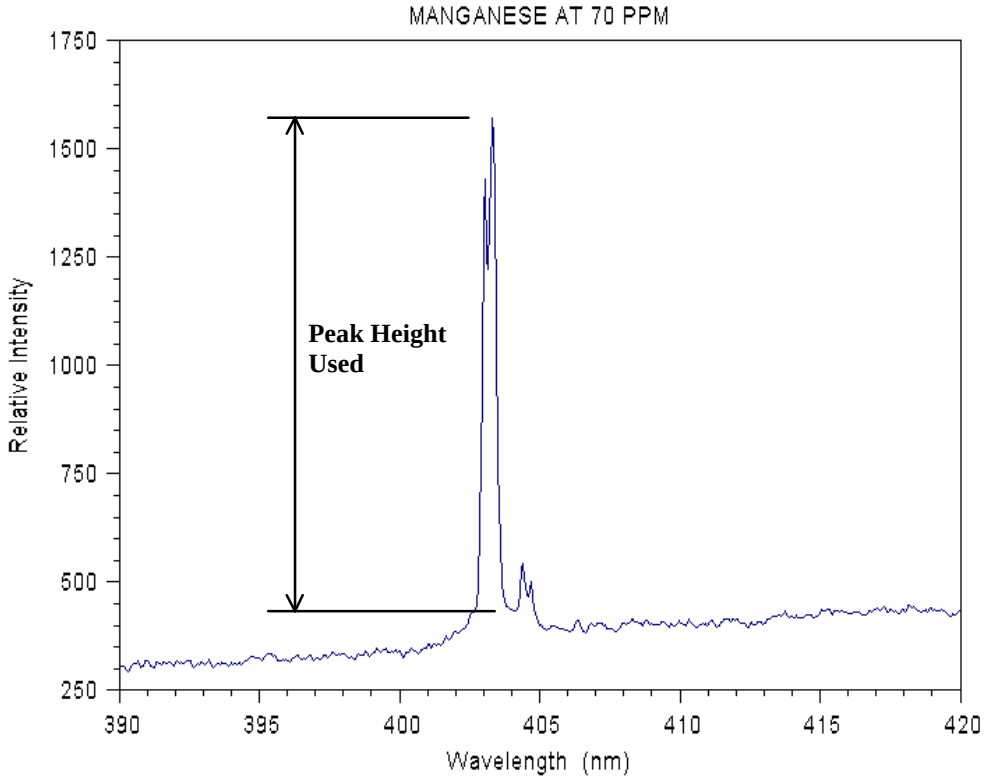

Figure 12. Measurement of Peak Height.

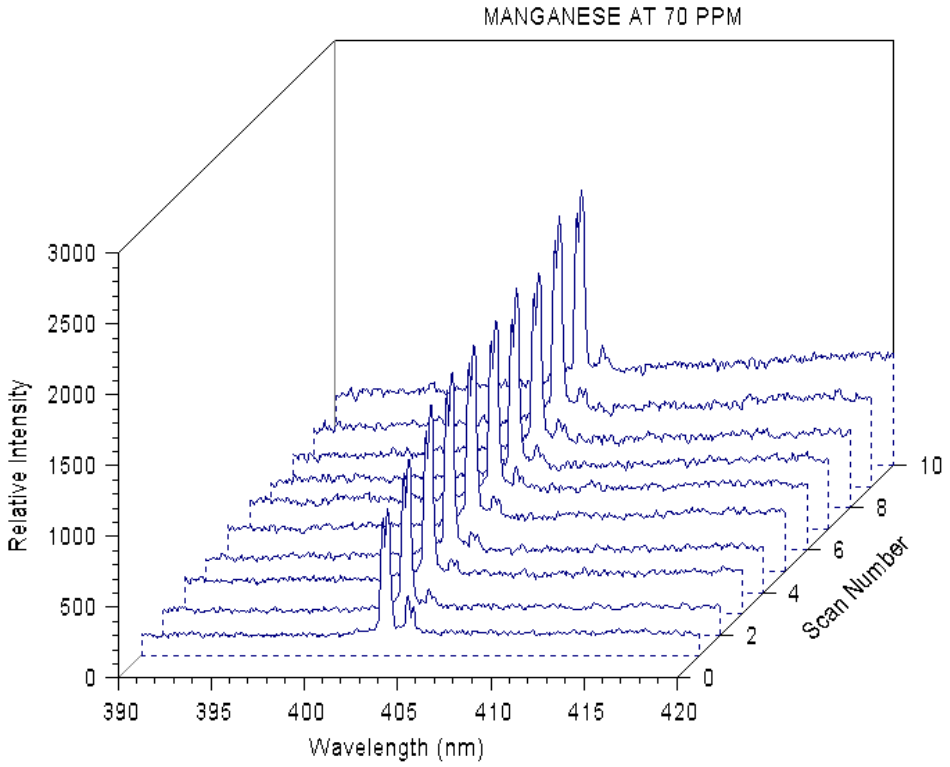

Figure 13. Data Collection for the 70 ppm Manganese Fuel Grain.

Table 2. Data from Qantitative Study.

Peak#	5 ppm	10 ppm	15 ppm	22 ppm	40 ppm	55 ppm	70 ppm	85 ppm	91 ppm
1	140	135	483	482	667	759	845	1,050	730
2	213	198	583	609	762	940	1,013	1,131	1,070
3	289	239	647	633	760	988	1,172	1,048	1,158
4	339	299	685	666	780	1,050	1,227	1,060	1,084
5	257	323	581	650	784	950	1,167	1,114	1,293
6	245	346	471	577	853	939	1,164	1,175	1,165
7	314	318	574	591	863	957	1,222	1,284	1,327
8	331	327	527	686	1,005	968	1,160	1,270	1,463
9	232	340	583	677	918	1,072	1,317	1,148	1,499
10	226	405	605	631	1,051	1,060	1,252	1,119	1,500
Avg. mid 6	296	309	580.83	633.83	840.83	975.33	1,185.33	1,158.5	1,248.33
Max.	339	346	685	686	1,005	1,050	1,227	1,284	1,463
Min.	245	239	471	577	760	939	1,160	1,048	1,084

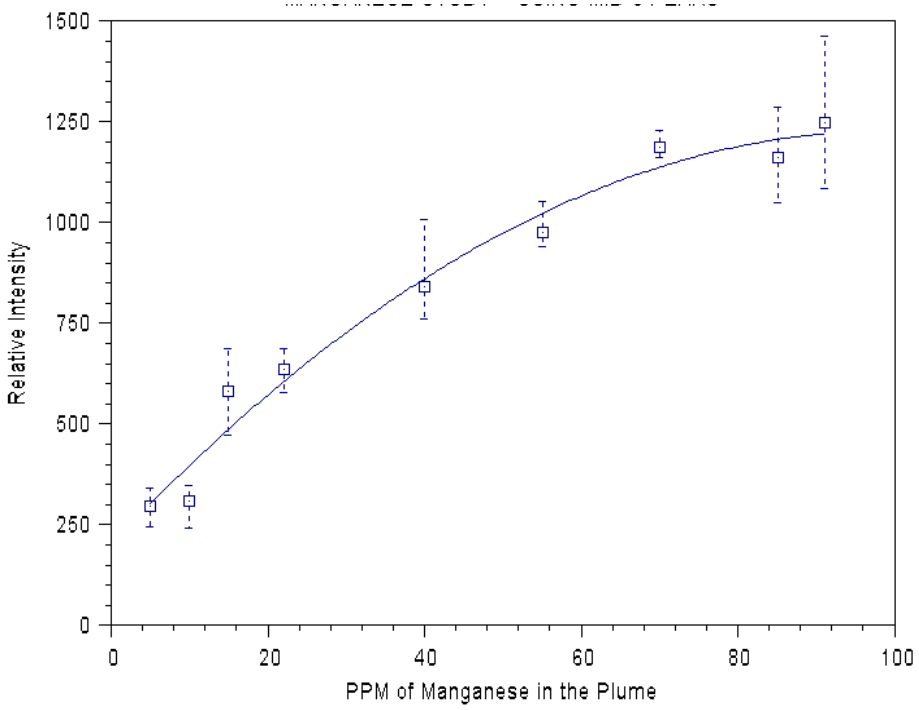

Figure 14. Final Results of the Manganese Quantitation Study.